

Climate change scenarios for the California region

Daniel R. Cayan · Edwin P. Maurer ·
Michael D. Dettinger · Mary Tyree · Katharine Hayhoe

Received: 2 August 2006 / Accepted: 5 October 2007 / Published online: 26 January 2008
© Springer Science + Business Media B.V. 2007

Abstract To investigate possible future climate changes in California, a set of climate change model simulations was selected and evaluated. From the IPCC Fourth Assessment, simulations of twenty-first century climates under a B1 (low emissions) and an A2 (a medium-high emissions) emissions scenarios were evaluated, along with occasional comparisons to the A1fi (high emissions) scenario. The climate models whose simulations were the focus of the present study were from the Parallel Climate Model (PCM1) from NCAR and DOE, and the NOAA Geophysical Fluid Dynamics Laboratory CM2.1 model (GFDL). These emission scenarios and attendant climate simulations are not “predictions,” but rather are a purposely diverse set of examples from among the many plausible climate sequences that might affect California in the next century. Temperatures over California warm significantly during the twenty-first century in each simulation, with end-of-century temperature increases from approximately +1.5°C under the lower emissions B1 scenario in the less responsive PCM1 to +4.5°C in the higher emissions A2 scenario within the more responsive GFDL model. Three of the simulations (all except the B1 scenario in PCM1) exhibit more warming in summer than in winter. In all of the simulations, most precipitation continues to occur in winter. Relatively small (less than ~10%) changes in overall precipitation are projected. The California landscape is complex and requires that model information be parsed out onto finer scales than GCMs presently offer. When downscaled to its mountainous terrain, warming has a profound influence on California snow accumulations, with snow losses that increase with warming. Consequently, snow losses are most severe in projections by the more responsive model in response to the highest emissions.

D. R. Cayan (✉) · M. D. Dettinger · M. Tyree
Scripps Institution of Oceanography, University of California, San Diego, La Jolla, CA, USA
e-mail: dcayan@ucsd.edu

D. R. Cayan · M. D. Dettinger
U.S. Geological Survey, La Jolla, CA, USA

E. P. Maurer
Santa Clara University, Santa Clara, CA, USA

K. Hayhoe
Department of Geosciences, Texas Tech University, Lubbock, TX, USA

1 Introduction

In May 2005, the California Energy Commission and the California Environmental Protection Agency (Cal/EPA) commissioned a report describing the potential impacts of twenty-first century climate changes on key state resources. Although precise prediction of the future climate is impossible, selected scenarios representative of possible climate changes, targeted regionally on California, were explored. This study was guided by previous and ongoing efforts by the Intergovernmental Panel on Climate Change (IPCC) (Houghton et al. 2001), an examination of ecological and related changes in California (Field et al. 1999), the U.S. National Climate Change Assessment (National Assessment Synthesis Team 2001), and the recent United Kingdom Climate Impacts Programme (http://www.ukcip.org.uk/resources/publications/documents/UKCIP02_briefing.pdf). Because of resource constraints and a short timeframe during which this report was completed, the present study focused on a small set of climate scenarios.

This work also builds upon previous climate model-based studies of possible climate change impacts on various sectors in the California region. These studies include a broad assessment of possible ecological impacts by Field et al. (1999); an assessment of a range of potential climate changes on ecosystems, health and economy in California described by Wilson et al. (2003); a study of how a “business-as-usual” emissions scenario simulated by a low sensitivity climate model would affect water resources in the western United States, overviewed by Barnett et al. (2004); and a multisectoral assessment of the difference in impacts arising from high vs. low greenhouse gas (GHG) emission in Hayhoe et al. (2004; hereafter designated H04).

Global and regional climates have already begun changing, probably from accumulating emissions of anthropogenic greenhouse gases. As reported by the WMO (2005), “since the start of the 20th century, the global average surface temperature has risen between 0.6°C and 0.7°C. But this rise has not been continuous. Since 1976, the global average temperature has risen sharply, at 0.18°C per decade. In the northern and southern hemispheres, the 1990s were the warmest decade with an average of 0.38°C and 0.23°C above the 30-year mean, respectively.” The 10 warmest years for the earth’s surface temperature all occurred after 1990 (Jones and Palutikof 2006) and 2005 was either the second or first warmest year on record (Jones and Palutikof 2006; Hansen et al. 2006). Much of the warming during the last four decades is attributable to the increasing atmospheric concentrations of GHGs due to human activities (Santer et al. 1996; Tett et al. 1999; Meehl et al. 2003). At the regional scales of California and western North America, signs of changing climate are also evident, in part reflecting the global changes noted above. Over the past 50 years, a set of observations suggest (though not conclusively) that climate warming may be operating in the California region. These include a trend toward warmer winter and spring temperatures (e.g., Cayan et al. 2001), smaller fractions of precipitation falling as snow instead of rain (Knowles et al. 2007), a decline in spring snow accumulations in lower and middle elevation mountain zones (Mote et al. 2005), an advance of snowmelt by 5 to 30 days earlier in the spring (Stewart et al. 2005), and a similar advance in the timing of spring flower blooms (Cayan et al. 2001).

An ongoing effort by the international climate-science community to prepare the Fourth IPCC Climate Change Assessment provided important background and crucial inputs for the studies reported here. In particular, that international assessment prompted and provided (through the Lawrence Livermore Laboratory Program for Climate Model Diagnosis and Intercomparison) a large number of climate model simulations of climates under selected GHG emission scenarios. The present effort has focused on just a few of the IPCC

simulations in order to provide concrete examples of possible impacts. Additionally, in more selective fashion, we analyze the large ensemble of projections generated for the IPCC assessment for perspectives on the scenarios selected for intense study in terms of two major sources of climate-change uncertainty: our incomplete understanding of how the climate system responds (as represented by differences between different climate models) and the unknowable future of emissions of GHGs and other contaminants to the atmosphere (as represented by the emissions scenarios considered here).

This paper describes, from California's perspective, the selection of climate models, emission scenarios, and downscaling methods used in the overall study. In particular, it examines differences among projections, and differences among historical to projected climates in the selected model runs. Additionally, for some analyses, it compares results within a larger ensemble of IPCC4 projections.

2 Scenarios and models

The climate models considered in this effort were among those that were prepared and evaluated by the IPCC. These include several models used in the IPCC Third Assessment (Cubasch et al. 2001), and several being used in the (presently) ongoing IPCC Fourth Assessment. A discussion of projections of climate change by climate models is presented by Cubasch et al. (2001) as part of the Third IPCC Climate Change Assessment. For this study, primary criteria for model selection were that the ocean and atmosphere components be freely coupled, i.e., not requiring or using flux-correcting formulations. The models considered were required to have an atmospheric grid spacing of 250 km or less. Another criteria for model selection was the availability of daily output data.

Models selected for attention here also were required to produce a realistic simulation of aspects of California's recent historical climate – particularly the distribution of monthly temperatures and the strong seasonal cycle of precipitation that exists in the region. In addition, models selected were required to contain realistic representations of some regional features, such as the spatial structure of precipitation. Because the observed California climate has exhibited considerable natural variability at seasonal to interdecadal time scales, the historical simulations by the climate models were required to contain variability that resembles that from observations at these short period climatic time scales.

Finally, the selection of models was designed to include models with differing levels of sensitivity to GHG forcing. All these criteria, taken together, identified two global climate models (GCMs), the Parallel Climate Model (PCM; with simulations from NCAR and DOE groups; see Washington et al. 2000; Meehl et al. 2003) and the NOAA Geophysical Fluid Dynamics Laboratory (GFDL) CM2.1 model (Stouffer et al. 2006; Delworth et al. 2006; Knutson et al. 2006). In some parts of California's assessment activities, the UK Hadley Center HadCM3 model (Gordon et al. 2000; Pope et al. 2000) was also used; the simulations by that model were described in, and derived from, the H04 study.

The choice of GHG emissions scenarios focused on herein, A2 (medium-high) and B1 (low) emissions, was based upon implementation decisions made earlier by IPCC4 (Nakic'enovic' et al. 2000), and on availability of certain crucial outputs that varied from emissions scenario to scenario. In addition to the two scenarios primarily addressed herein, results from H04 based on a third scenario, A1fi (high emissions), was also used in some part of the overall assessment. These A1fi results are compared with selected results in the present study.

The B1 scenario assumes that global (including California) CO₂ emissions peak at approximately 10 gigatons per year (Gt/year) in mid-twenty-first century before dropping below current levels by 2100. This yields a doubling of CO₂ concentrations relative to its pre-industrial level by the end of the century, followed by a leveling of the concentrations (Fig. 1). Under the A2 scenario, CO₂ emissions continue to climb throughout the century, reaching almost 30 Gt/year. By the end of the twenty-first century, CO₂ concentrations reach more than triple their pre-industrial levels. The A1fi scenario has high emissions until about 2080, when they finally level off by Century's end. The A1fi emissions result in CO₂ concentrations that reach about 950 ppm in 2100.

Both the GFDL and PCM modeling groups performed historical simulations – under the so-called 20C3M conditions (see http://www-pcmdi.llnl.gov/projects/cmip/ann_20c3m.php), that allow us to compare global climate model performance to historical observations during late-nineteenth and entire-twentieth centuries. 20C3M runs for GFDL span 1861–2000 and for PCM span 1890–1999. The 20C3M conditions used in both models accounted for historical inputs into the atmosphere of aerosols from volcanic eruptions, changes in solar irradiance, and anthropogenic GHG and aerosol loadings (Delworth et al. 2006; Meehl et al. 2003). The 1961–1990 period of modeled climate was used in the present study as a climatology, a benchmark to which future-climate simulations were compared.

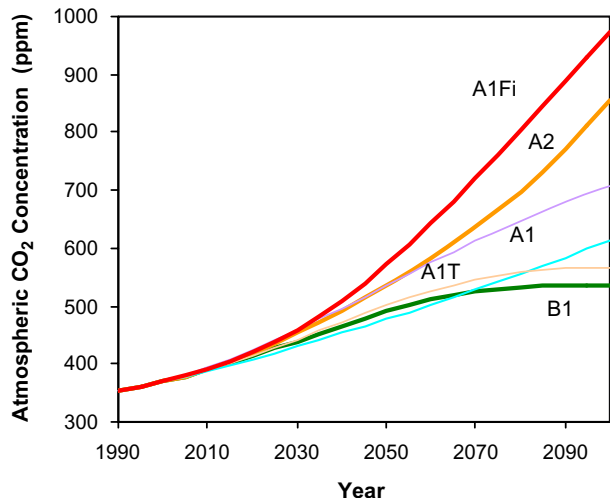
3 Climate model simulations: a California perspective

Most of the impacts considered in the California assessment are driven by changes in climate at the surface, so we focus on characteristics related to surface air temperature and precipitation in the region.

3.1 Temperature projections

Each of the model projections contains symptoms of global climate change over the California region. As we know from previous studies (e.g., H04, Dettinger 2005), there is more consistency among the various models and different simulations of individual models

Fig. 1 Projected atmospheric CO₂ concentrations under several of the IPCC emission scenarios



in the changes of some elements, such as temperature, than others, such as precipitation. Due to differences in the two models' parameterizations, sensitivities and responses to greenhouse gases and other forcings, there are substantial differences between the projections by the two models. PCM has relatively low sensitivity of global and regional temperature to GHG forcing and the GFDL model has a relatively high sensitivity, compared to the larger set of IPCC global climate models (Cayan et al. 2006). There also are significant differences between the two GHG emission scenarios that grow over time, an aspect of this problem that has been emphasized in previous studies (Houghton et al. 2001, H04.) and that is again an important theme in the present results. Northern California temperature warms significantly between 2000 and 2100, with trends ranging from approximately 1.5°C in the lower emissions B1 scenario within the less responsive PCM model to 4.5°C in the higher emissions A2 scenario within the more responsive GFDL model (see Tables 1 and 2). Temperature changes occur rather steadily through the twenty-first century, with annual temperature increases in Northern California reaching 1.5 and 0.5°C, respectively in the GFDL A2 simulation and the PCM B1 simulation as an average over 2005–2034. These same model projections reach a warming of 2.3 and 1.3°C as an average over 2035–2064; by mid-century the differences in GHG loading between the emissions scenarios begin to distinguish themselves. To put this warming into perspective, the projected Northern California temperature increase by the end of the twenty-first century (averaged over 2070–2099) for the B1 simulation is slightly larger than the differences in annual mean temperature between Monterey, a cool central California coastal location and Salinas, a warmer location approximately 15 km inland. For the A2 simulation, the warming by the end of the century is somewhat larger than the annual temperature difference between San Francisco, a cool coastal location and San Jose, a warm interior valley to the southeast sheltered from the ocean by the coast range. The present-day difference in annual mean temperatures between Monterey (18.5°C) and Salinas (19.9°C) is 1.4°C and the difference between San Francisco Mission Delores (17.6°C) and San Jose (21.7°C) is 4.1°C.

In both models, beyond the first three decades of the twenty-first century (Tables 1 and 2), warming is greater under the higher emission A2 scenario than under the lower emission B1

Table 1 Temperature and precipitation changes, GFDL and PCM B1 and A2 simulations, Northern California

NOCAL														
	Mean 1961–1990		2005–2034 change				2035–2064 change				2070–2099 change			
			GFDL		PCM		GFDL		PCM		GFDL		PCM	
	GFDL	PCM	A2	B1	A2	B1	A2	B1	A2	B1	A2	B1	A2	B1
Annual °C	9.3	8.0	1.5	1.4	0.5	0.5	2.3	2.2	1.3	.8	4.5	2.7	2.6	1.5
Summer °C (JJA)	21.5	17.9	2.1	1.7	0.9	0.6	3.4	2.6	1.7	1.1	6.4	3.7	3.3	1.6
Winter °C (DJF)	-0.46	0.08	1.4	1.3	0.1	0.7	1.7	2.1	0.9	2.4	3.4	2.3	2.3	1.7
Annual mm/%	1,098	750	+0.3	+2	-0.4	+7	-3	-2	-2	+3	-18	-9	-2	0
Summer mm/% (JJA)	14	14	-29	-6	+28	+44	-67	-13	+35	-18	-68	-43	-30	-4
Winter mm/% (DJF)	649	386	-1	+13	-5	+13	+6	-0.1	-5	-2	-9	-6	+4	+4

Temperature units are °C, precipitation in mm. Mean values are provided for historical (1961–1990) period, and changes between successive 30 year periods are shown in subsequent columns for the models/emission scenarios, as indicated. Units are °C for temperature means and changes, mm for precipitation means, and % for precipitation changes.

Table 2 Temperature and precipitation changes, GFDL and PCM B1 and A2 simulations, Southern California

SOCAL

	1961–2000		2005–2034 change				2035–2064 change				2070–2099 change			
			GFDL		PCM		GFDL		PCM		GFDL		PCM	
	GFDL	PCM	A2	B1	A2	B1	A2	B1	A2	B1	A2	B1	A2	B1
Annual °C	12.2	14.3	1.3	1.3	0.5	0.6	2.3	2.1	1.2	0.8	4.4	2.7	2.5	1.6
Summer °C (JJA)	23.2	23.4	1.7	1.6	0.4	0.5	3.1	2.3	1.3	0.8	5.3	3.2	2.6	1.5
Winter °C (DJF)	2.4	5.4	1.0	1.0	0.2	0.7	1.7	1.6	1.0	0.6	3.3	2.0	2.4	1.6
Annual mm/%	537	342	-6	-2	+7	+18	-2	-11	+7	-2	-26	-22	+8	+7
Summer mm/% (JJA)	7	5	+49	-13	-7	+6	-60	-50	+35	+33	-44	-63	-11	+2
Winter mm/% (DJF)	320	187	-0.7	+0.8	+1	+32	+9	-9	+6	-6	-2	-26	+8	-0.8

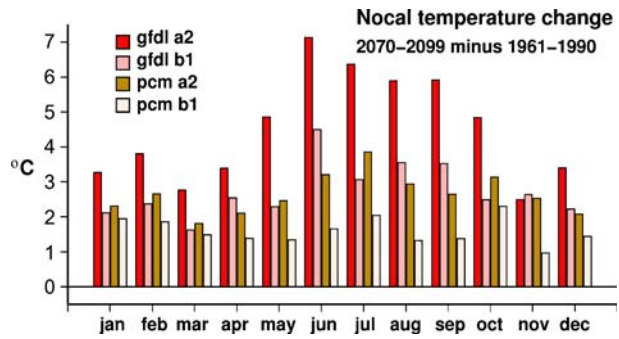
Temperature units are °C, precipitation in mm. Mean values are provided for historical (1961–1990) period, and changes between successive 30 year periods are shown in subsequent columns for the models/emission scenarios, as indicated. Units are °C for temperature means and changes, mm for precipitation means, and % for precipitation changes.

scenario. The warming during the twenty-first century is approximately linear in each of the model runs, although there are substantial year to year variations in temperature associated with the normal climate variations on a variety of time scales. Additionally, projected warming in the A1fi simulations by PCM (H04) were greater than those in the A2 simulations examined here, yielding 3.8°C warming in A1fi (Tables 1 and 2 of H04) compared to 2.7°C warming in A2, as shown in Tables 1 and 2. This additional A1fi warming is roughly proportionate to the greater GHG concentrations by end of century in this more extreme scenario.

Three of the simulations (all except the PCM B1 projection) yield more warming in summer than in winter, as shown for a northern California location in Fig. 2. In the high emission A2 projections for northern California, mean temperatures increase by the end of the twenty-first century by 2.6 and 5.3°C in summer and 2.4 and 3.3°C in winter, in the PCM and GFDL models respectively. Inspection of larger scale patterns of the model simulations indicates that the accentuation of warming in summer is common to all continental areas, and may be affected by earlier and greater drying of continental land surfaces (Gershunov and Douville 2007). If the projected summer amplification of warming occurs, it has important implications for impacts such as ecosystems, agriculture, water and energy demand, and the occurrence of heat waves, which can have consequences for public health and the economy.

In the 30 years from 2005–2034, warming – even in PCM under B1 – amounts to more than 0.5°C in winter and summer. Already, this near-term warming is sufficient to reduce (increase) substantially the number of cold (warm) days in summer and winter, effectively eliminating summers that fall into the cool third of the temperature distribution in the GFDL projections (Fig. 3). By the 30 years from 2070–2099, under all the scenarios considered here (including A1fi from H04,) northern California summer temperatures increase in GFDL projections by 6.4°C under A2 and 3.6°C under B1. In the last parts of the twenty-first century, counts of northern California seasonal temperatures falling below the lower historical tercile and above the upper tercile reveals a remarkable change (Fig. 3). By 2070–2099, in all of the model runs (except PCM B1), seasonal mean temperatures in the lower third of the historical distribution have been eliminated, and in the PM B1 projection, no

Fig. 2 Projected changes in monthly-mean temperatures in northern California during 2070–2099, and relative to 1961–1990, for PCM and GFDL B1 and A2 simulations



more than two winters and one summer fall into the lowest third in any decade. Also, the warming greatly reduces the number of seasonal temperatures in the climatological normal category (between the lower and upper terciles) at the expense of large, almost unanimous, increases into the warmest third of the distribution.

The shift in the distribution of seasonal temperatures is mirrored by a similar shift in daily temperatures. The occurrence of extremely warm daily mean temperatures, exceeding the 99.9 percentile of their historical distributions for the June–September summer months, tallied for the PCM and GFDL A2 simulations (Table 3, upper), increases to 50–500 times their historical frequency by 2070–2099. Conversely, the incidence of even moderately cool daily mean winter temperatures decreases markedly (Table 3, lower).

As might be expected from the large thermal capacity of the ocean relative to land, the air temperature change just above the sea surface along the California coast is less than that above the adjacent land surface. This change, which represents an enhancement of the present-day coast-inland temperature gradient, is illustrated in Fig. 4, showing the air temperature warming (2070–2099 vs. 1961–1990) in summer (June–August) in A2 simulations by GFDL and PCM in grid points from the PCM and GFDL models,

Fig. 3 Occurrence of seasonal temperatures falling into coolest (blue) and warmest (red) thirds of their historical (1961–1990) distribution for PCM and GFDL simulations, under A2 and B1 emission scenarios. Values plotted are counts in 10-year moving windows with the bars centered in each window

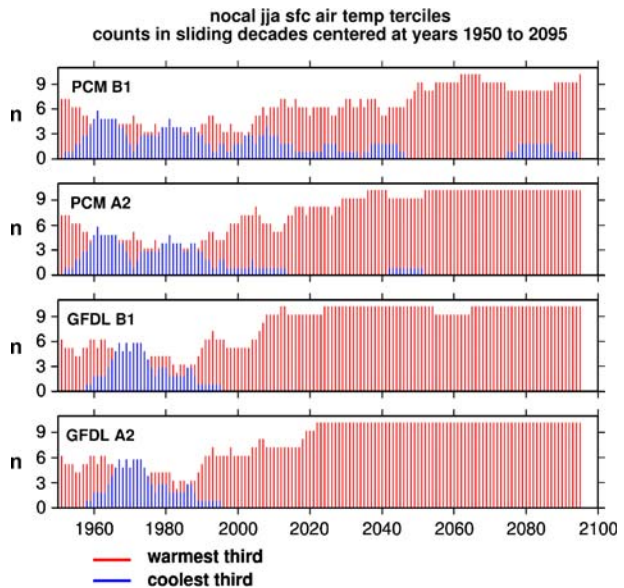


Table 3 Daily extreme (99.9th % ile) temperature occurrences June–September

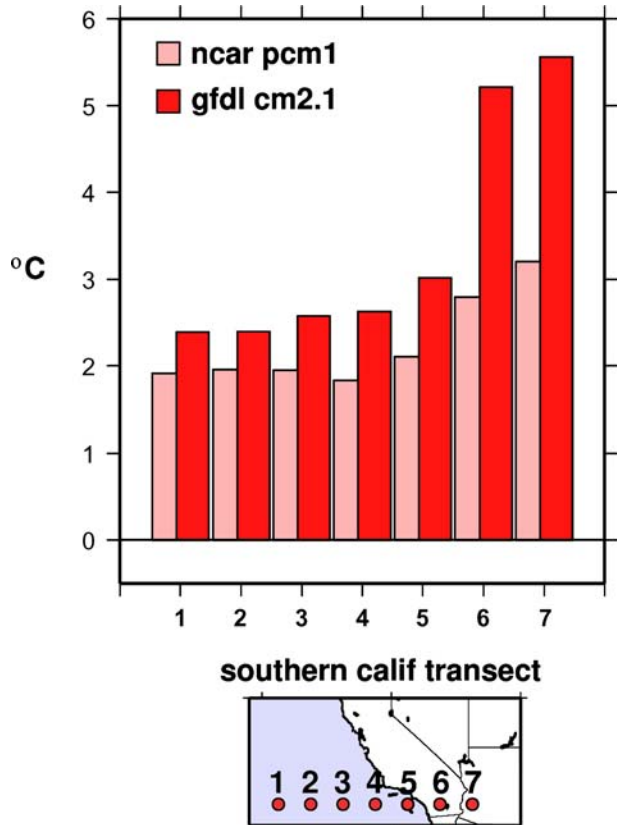
	No Cal				So Cal			
	PCM		GFDL		PCM		GFDL	
	B1	A2	B1	A2	B1	A2	B1	A2
1961–1990	4	4	4	4	4	4	4	4
2005–2034	15	39	53	111	7	13	13	10
2035–2064	43	80	165	227	8	18	27	39
2070–2099	56	258	210	856	24	59	52	228

respectively, traversing a swath from coastal ocean to land across southern California. The warming of surface air increases markedly, increasing from 1.8 to 3.2°C in PCM and from 2.3 to 5.5°C in GFDL. Results are very similar in an analogous ocean-land transect traversing central California.

3.2 Precipitation projections

The Mediterranean seasonal precipitation regime in California is not projected to change noticeably. This is indicated by the monthly mean precipitation for the B1 and A2

Fig. 4 Change in June–August temperatures (2070–2099 minus 1961–1990) for PCM and GFDL A2 simulations along a transect of model locations (shown in *inset*) from the offshore ocean and to interior land in Southern California. In both models, grid “squares” 1–4 are comprised entirely of ocean surface, grid squares 6 and 7 are comprised entirely of land surface, and grid square 5 is partly land and mostly ocean surface



simulations from PCM and GFDL over northern California, southern central California, and southern California in Fig. 5. In all simulations, most precipitation over northern California and southern central California continues to occur in winter. In the PCM historical and climate change simulations, climatological precipitation in southern California exhibits a fall peak (notably in the southern part of the state as shown in “southern California” on the bottom panels of Fig. 5), which is not in agreement with the strong winter season Mediterranean precipitation regime observed there. Summer precipitation changes only incrementally, and actually decreases in some of the simulations, so there is no simulated consensus of a stronger thunderstorm activity.

The projections from both models were characterized by relatively modest trends in mean precipitation during the 2000–2100 period (Tables 1 and 2). In Northern California, by end of century, projected precipitation increases slightly or does not change in one model (PCM), and decreases by 10–20% in the other model (GFDL). Analysis of California precipitation changes produced under B1 and A2 emissions scenarios in 11 global climate models by Maurer (2007) also finds only modest changes in annual precipitation, but with some increases in precipitation in winter months and decreases in spring months; our analyses of the larger set of IPCC model runs has hints of these seasonal tendencies, but only marginally. The small annual precipitation changes are consistent with the fact that although, in general, under global warming, global rates of precipitation are projected to increase, these increases tend to be geographically focused in the tropics and higher latitude extra-tropics. In most current projections of global warming, subtropical and lower middle latitude regions exhibit little change in precipitation and in some cases become drier.

Although little change (often in the form of small decreases) in northern Californian precipitation is projected during the twenty-first century, there is a modest tendency for increases in the numbers and magnitudes of large precipitation events. This increase is

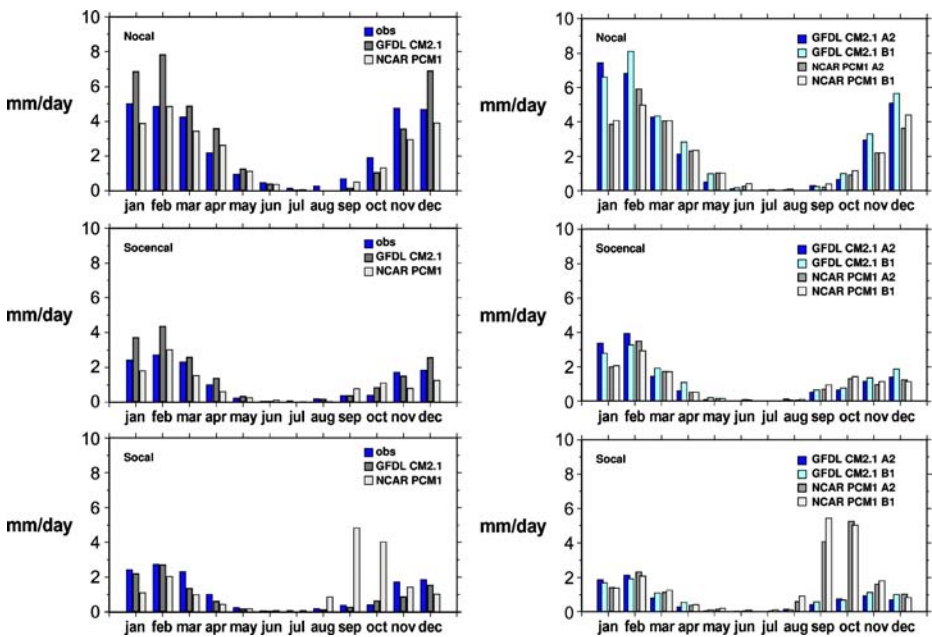


Fig. 5 Historical (1961–1990, *left*) observed and simulated precipitation, and projected (2070–2099, *right*) average monthly precipitation, Northern California, south Central California, and Southern California

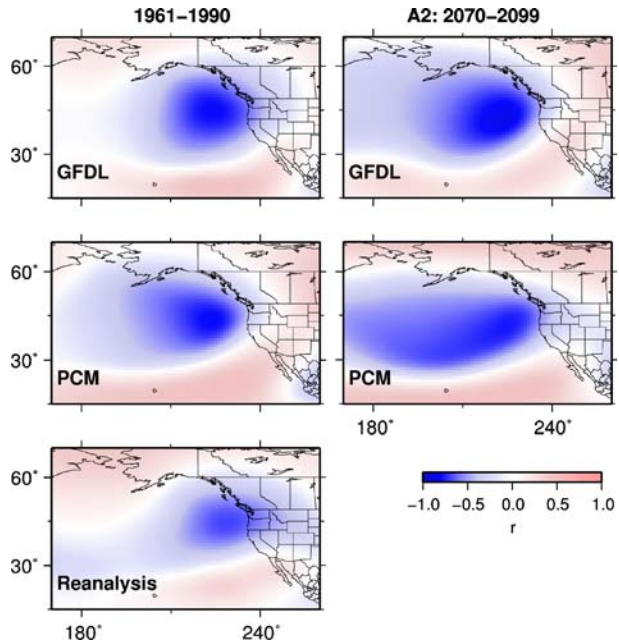
Table 4 Daily extreme precipitation occurrences, PCM and GFDL A2 simulations

	No Cal				So Cal			
	PCM		GFDL		PCM		GFDL	
	99% ile	99.9% ile	99% ile	99.9% ile	99% ile	99.9% ile	99% ile	99.9% ile
1961–1990	111	12	111	12	111	12	111	12
2005–2034	117	8	129	19	129	19	93	12
2035–2064	129	14	130	40	130	40	129	7
2070–2099	161	25	127	30	127	30	98	10

illustrated in Table 4 by the number of daily precipitation events falling into the 99.0 and 99.9 percentiles compared to the corresponding frequencies in the historical-period simulations from the same GCMs.

Similar to observations, precipitation in the projections exhibits considerable monthly to interdecadal variability. The anomalous atmospheric circulation patterns in the simulations that produce much of the precipitation variability are quite similar to those in nature. Winter season precipitation is mostly derived from North Pacific winter storms, as demonstrated by comparing the correlations between Northern California monthly precipitation and 500 HPa height (500 millibar height), mapped over the Pacific and western North America domain for the 1960–1991 and 2070–2099 periods from the A2 simulations of GFDL and PCM, to the correlation in observations (Fig. 6). The models also exhibit a significant El Nino/Southern Oscillation signal from interannual sea surface temperature (SST) variations in the tropical NINO 3.4 region (Cayan et al. 2006). These SST variations are teleconnected to anomalous storm activity in the North Pacific and western North America storm activity, with the warm (El Nino) phase favoring a wetter pattern in southern California and the

Fig. 6 Correlations between Nov–Mar mean precipitation, Northern California, and Nov–Mar 500HPa height anomalies at each point in Pacific-western North America domain for the historical period (1961–1990, left) and for 2070–2099 (right) in GFDL and PCM A2 simulations, and for observations from NCAR/NCEP Reanalysis

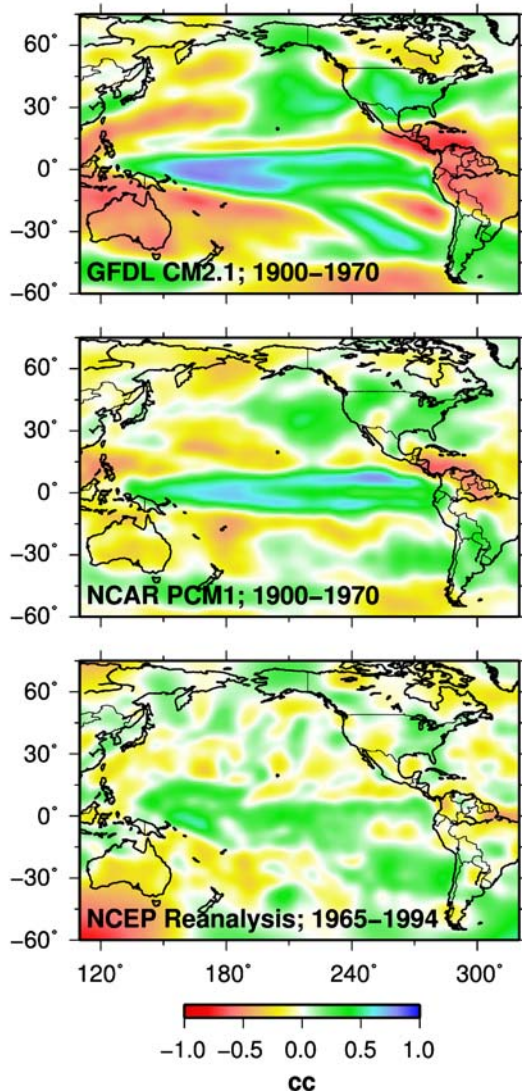


Southwest and the cool (La Nina) phase favoring drier conditions there (e.g. Dettinger et al. 2001). The models, to a fair degree, replicate this pattern, illustrated in Fig. 7. In the model projections of twenty-first century climate, the frequency of warm tropical events (El Niños) remains about the same as in the historical simulations, and model El Niño events continue to be related to anomalous precipitation patterns over California.

Simulated interannual-to-interdecadal variability of precipitation and temperature is prominent and inspection of plots of the temperature and precipitation data indicate that this variability does not change much from the historical period of the simulations to the climate change simulation of the twenty-first Century. This is evident from plots of ensembles of the same model and same scenario, simply run in perturbed fashion using different initial

Fig. 7 Correlation between Nino 3.4 SST and precipitation across the globe from simulations by GFDL (*above*) and PCM (*middle*), along with observations from NCEP/NCAR Reanalysis (<http://www.cdc.noaa.gov/cdc/reanalysis/reanalysis.shtml>; *below*) demonstrate strong connection between tropical Pacific ENSO fluctuations and extratropical precipitation

Nino3.4 SST vs annual precip on global grid



conditions (Fig. 8). This non-trending, shorter period variability is important because large impacts are most likely to occur when secular changes are superimposed on (generally larger) short period variations to cause extreme phenomena such as floods, drought, and heat waves. An ensemble of simulations, accomplished by seeding the model simulations with differing initial conditions, for historical conditions and for a given GHG emission scenario, provides a measure of the internal variability of a particular climate model. The intra-scenario variability for the two models is fairly high, as seen in the set of historical and climate change simulations of annual precipitation in Fig. 8. Similar variability, albeit superimposed on a rising trend, are exhibited by a set of ensembles of winter and summer temperature from the PCM A2 simulation (not shown). The projected trends occur in the context of the seemingly unaltered occurrence of this (simulated) natural variability.

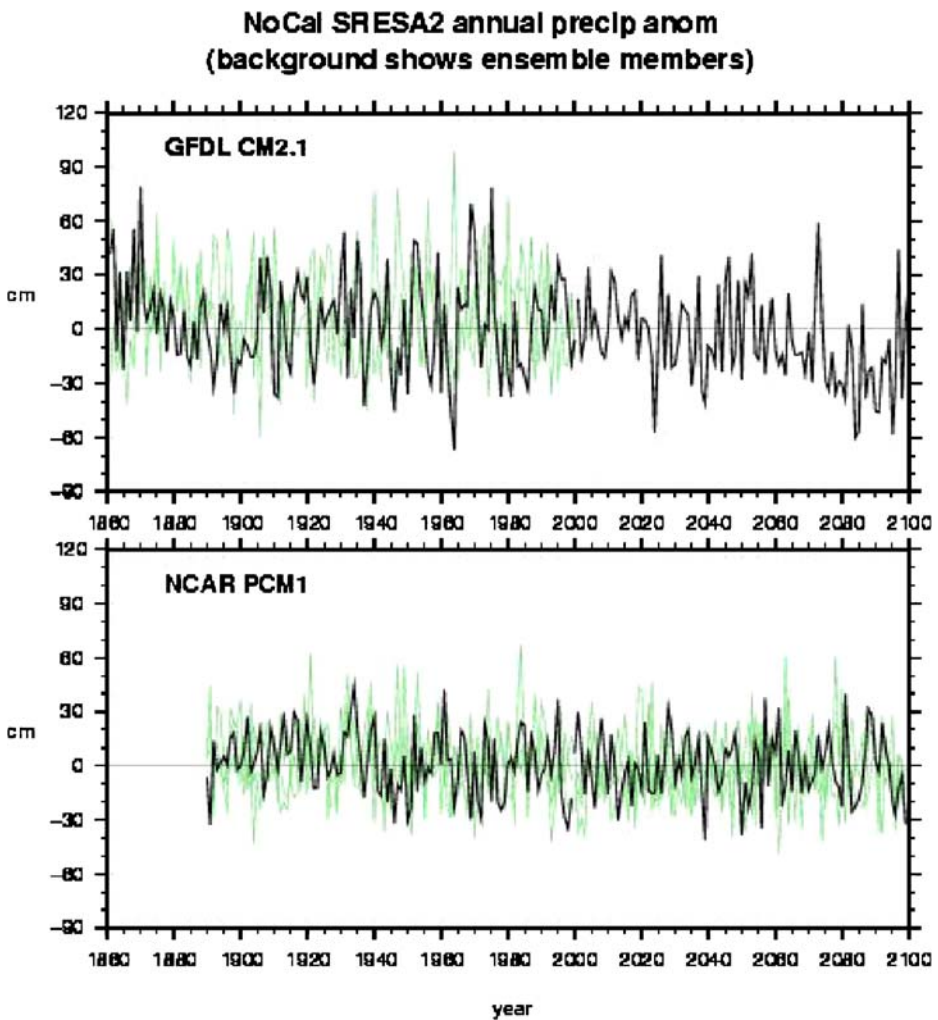


Fig. 8 Ensemble of Northern California precipitation projections from multiple simulations by GFDL (*top*) and PCM (*bottom*) models under historical and A2 conditions, with the specific runs analyzed herein highlighted

To put the two scenarios and the two GCMs that are the focus of this assessment into broader perspective, it is useful to compare them with projections of climate changes over California from the larger collection of simulations. Following an analysis by Dettinger (2005, 2006), projection distributions were estimated for a much larger subset of the Fourth IPCC Assessment simulations, including 84 simulations from a total of 12 different climate models responding to three different emission scenarios: higher (A1b), middle-high (A2), and low (B1). This large ensemble of simulations describes a range of projected temperature anomalies in the 2070–2099 period, all positive, from relatively modest to quite large (e.g., from about +2 to +7°C). The distribution of precipitation totals includes both positive and negative anomalies that cluster with moderate change around present-day averages and with modest increases in the range of precipitation variability and differences within the ensemble, shown in Tables 1 and 2 and in univariate (Fig. 9) and joint (Fig. 10) distributions of temperature and precipitation.

Throughout the 100 year simulation, Northern California conditions projected by PCM remain in the lower half of the temperature distributions, exhibiting a relatively modest degree of warming (Fig. 11). The small changes experienced by PCM B1 and A2 are close to the center of the overall precipitation distributions. In contrast, Figs. 9 and 10 shows that California temperatures projected by GFDL and HadCM3 (from H04) are in the warmer half of the overall temperature distributions. GFDL and HadCM3 projections of precipitation tend to be in the drier parts of the precipitation distributions. The projected precipitation changes are not correlated with the temperature changes overall, as shown by

Fig. 9 Distribution of anomalies (curves, relative to 1961–1990 means) of Northern California annual temperature (in °C, above) and precipitation (in %, below) constructed by a sampling technique (Dettinger 2005) applied to an 84-member ensemble of IPCC 4th Assessment projections from 12 models responding to three GHG emission scenarios,. Symbols indicated 30-year mean projected changes in various projections discussed here

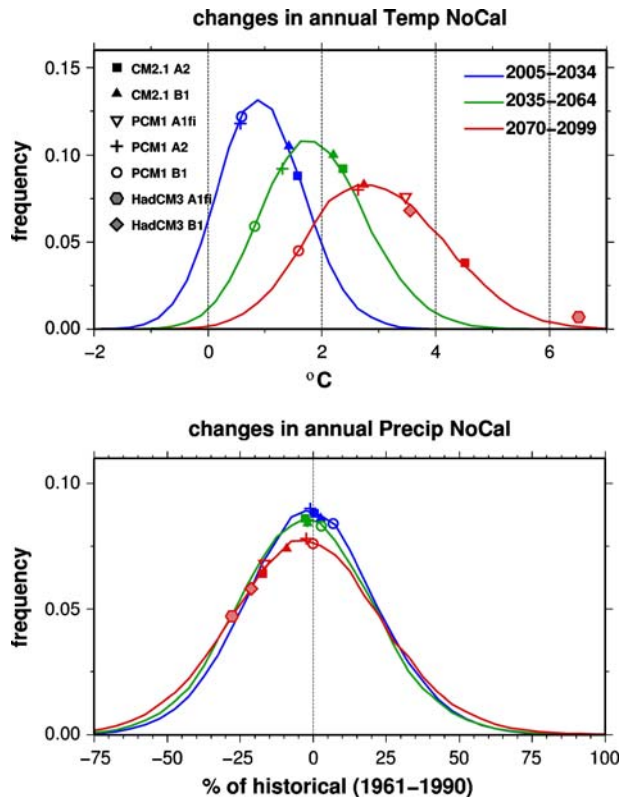
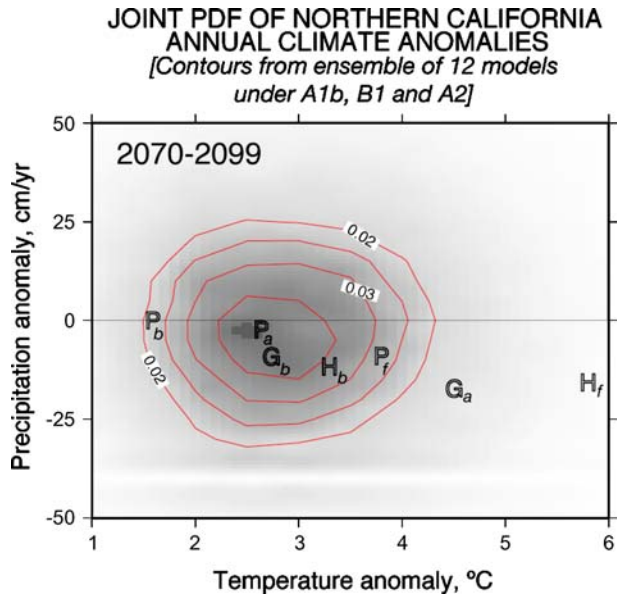


Fig. 10 Joint probability distribution of annual temperature and precipitation anomalies, 2070–2099, relative to 1960–1999 means, constructed from the IPCC4 ensemble described in caption of Fig. 9. *P*, *G*, and *H* designate 30-year mean changes from PCM1, GFDL 2.1 and HadCM3 models; *b*, *a*, *f* designates B1, A2 and A1fi GHG scenarios



the joint probability of temperature and precipitation changes in Fig. 10. If they were, then warming-moistening or warming-drying trends might become systematic parts of the projection ensemble. If they were a feature of the IPCC4 projections, such combinations of trends would certainly influence the kinds of snowmelt and streamflow responses that follow. Because these combinations occur only randomly in the ensemble, projected precipitation changes (such as they are) and temperature changes are almost independent from model to model, and snowmelt processes must be assessed projection by projection.

4 Reductions in snow accumulation

The selection of GCMs for this study required that they exhibit, on a broad spatial scale, seasonal patterns of simulated precipitation and temperature for the historic period that

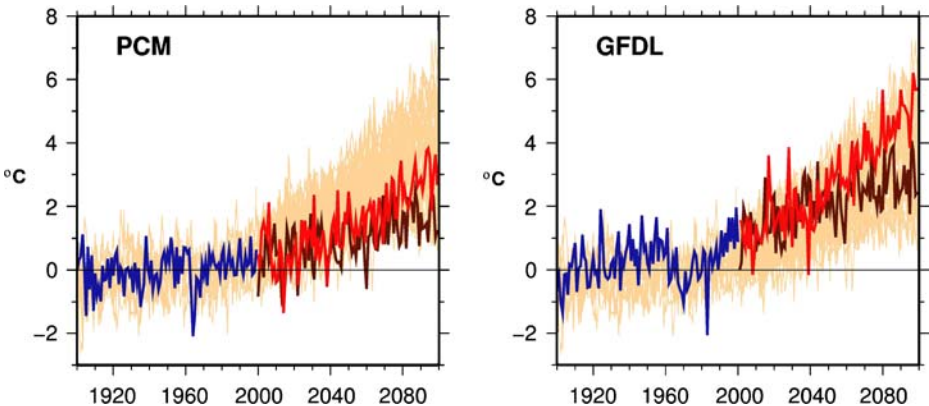


Fig. 11 Time series of northern California temperature projections from 39 AR4 simulations with PCM (left) and GFDL (right), with the historical, B1 and A2 simulations analyzed here highlighted

resemble those in nature. However, many climate impacts arise from finer-grained phenomena, often influenced by topographic features, e.g., notably, the winter and spring snow accumulation in California, which occurs primarily in mountain catchments. Also, even the best models display biases on regional scales that are large enough that the impacts of climate change may be difficult to trace from large-scales to the scales of landscapes and watersheds.

To correct systematic bias in the models and to interpolate the climate changes to scales comparable with topography and landscape, in this study, we employed a statistical bias correction technique and downscaling technique originally developed by Wood et al. (2002) for using global model forecast output for long-range streamflow forecasting. This technique was later adopted to downscale GCM output for use in studies examining the hydrologic impacts of climate change (H04; Maurer and Duffy 2005; Payne et al. 2004; VanRheenen et al. 2004). This is an empirical statistical technique that maps GCM precipitation and temperature during a historical period (1950–1999 for this study) to the concurrent historical observed record, which for this study is taken to be a gridded National Climatic Data Center Cooperative Observer station data set (Maurer et al. 2002). This observed data set, developed at a spatial scale of $1/8^\circ$ (about 7 mi or 12 km), was aggregated to a 2° latitude-longitude spatial resolution.

The combined bias correction/spatial downscaling method used in this study has been shown to compare favorably to different statistical and dynamic downscaling techniques (Wood et al. 2004) in the context of hydrologic impact studies. For precipitation and temperature, cumulative distribution functions (CDFs) are built for each of 12 months for each of the 2° grid cells for both the gridded observations and each GCM (first interpolating raw GCM data onto a common 2° grid) for the historical period (1950–1999). GCM quantiles are then mapped onto the climatological CDF for the entire simulation period. For example, if precipitation at one grid point from the GCM has a value in January of 2050 equal to the median GCM value (for January) for 1950–1999, it is transformed to the median value of the January observations for 1950–1999. For temperature, the linear trend is removed prior to this bias correction step, and is replaced afterward, to avoid increasing sampling at the tails of the CDF as temperatures rise. Thus, the probability distributions of the observations are reproduced by the bias corrected climate model data for the overlapping historical period, while both the mean and variability of future climate can evolve according to GCM projections.

The GFDL model has a resolution (of the atmospheric component) of 2.5° longitude by 2.0° latitude (approximately 137×137 mi (220×220 km) per grid cell), and the PCM uses a standard T42 resolution (approximately 2.8° , or 155×186 mi (250×300 km) in California). The spatial scale of the GCMs is very large compared to the scale of interest for many impact studies. For example, the area of one GCM atmospheric grid cell (simulated essentially as one area of constant elevation and land surface condition) is more than 10 times as large as the entire American River basin upstream of Folsom Dam. The Wood et al. (2002) statistical method interpolates the bias corrected GCM anomalies, expressed as a scale factor (for precipitation) and shift (for temperature) relative to the climatological period at each 2° GCM grid cell to the centers of $1/8$ degree grid cells over California. These factors are then applied to the $1/8$ degree gridded historical precipitation and temperature (examples shown in H04 and Cayan et al. 2006).

To generate supplemental meteorological data that drives snow accumulation (such as radiative forcing, humidity, etc.) as well as to derive land surface hydrological variables consistent with the downscaled forcing data, the variable infiltration capacity (VIC) model (Liang et al. 1994, 1996) was used. VIC is a macroscale, distributed, physically based

hydrologic model that balances both surface energy and water over a grid mesh, and has been successfully applied at resolutions ranging from a fraction of a degree to several degrees latitude by longitude. The VIC model includes a “mosaic” land surface scheme, allowing a statistical representation of the sub-grid scale spatial variability in topography and vegetation/land cover. This is especially important when simulating the hydrologic response in complex terrain and in snow dominated regions. To account for subgrid variability in infiltration, the VIC model uses a scheme based on work by Zhao et al. (1980). The VIC model also features a nonlinear mechanism for simulating slow (baseflow) runoff response, and explicit treatment of a vegetation canopy on the surface energy balance. Following the simulation of the water and energy budgets by the VIC model, a second program is used to route the derived runoff through a defined river system to obtain streamflow at specified points. The algorithm used in this study, developed by Lohmann et al. (1996), has since its development been employed in all simulations of streamflow using output from the VIC model. The VIC model has been successfully applied in many settings, from global to river basin scale (Abdulla et al. 1996; Maurer et al. 2001; Maurer et al. 2002; Nijssen et al. 1997; Nijssen et al. 2001), as well as in several studies of hydrologic impacts of climate change (Christensen et al. 2004; H04; Maurer and Duffy 2005; Payne et al. 2004; Wood et al. 2004). For this study, the model was run at a 1/8-degree resolution (measuring about 150 km² per grid cell) over the entire California domain, including all land surface area between latitudes 32°N and 44°N and west of longitude 113°W. For deriving streamflows within the Sacramento-San Joaquin river basin the identical parameterization to VanRheenen et al. (2004) was used.

Although precipitation changes little or only modestly during the period of the climate simulations, climate warming is projected to reduce snow accumulation in California (Lettenmaier and Gan 1990; Knowles and Cayan 2002; Miller et al. 2003). This is because warming causes more of the precipitation to fall as rain and less as snow (Knowles et al. 2007). Such changes in precipitation type (more rain and less snow) are indicated by substantial changes in daily temperature during days with precipitation, shown in Fig. 12 for Northern California projections. Notably, minimum temperatures tend to be warmest during days with the heaviest precipitation. For each model and each emission scenario, all precipitation categories, including dry days, are warmer in 2070–2099 than the historical climatological distribution, with wetter days generally warming more than dry days.

During the historical period, snow accumulation has already exhibited losses of order 10% of April 1 snow water equivalent (SWE) across the western conterminous United States (Mote et al. 2005), and is expected to melt earlier as climate warming continues (Knowles and Cayan 2002; Wood et al. 2004; Maurer and Duffy 2005). Each of the climate simulations, when used as input to the VIC hydrologic model, yields substantial losses of spring snow accumulation over the Sierra Nevada. These losses become progressively larger as warming increases during the twenty-first century. The losses are also largest in projected responses to the simulated climates from the more sensitive model under the highest GHG emissions. As depicted in Table 5, and Figs. 13 and 14, the losses (negative) or gains (positive) of April 1 snow water equivalent (SWE) in the San Joaquin, Sacramento and Trinity drainages, as percentages of (1961–1990) historical averages, range from +6 to –29% (for the 2005–2034 period), from –12 to –42% (for 2035–2064), and from –32 to –79% (for the 2070–2099 period). The GFDL model, with its greater temperature sensitivity to increased GHG concentrations, produces snowpack losses about twice as large as those produced by the PCM. Most but not all of this difference can be ascribed directly to the projected warmings; the remainder is mostly due to the declining precipitation totals that GFDL projects. For both models, snowpack losses are greatest in the warmer, more

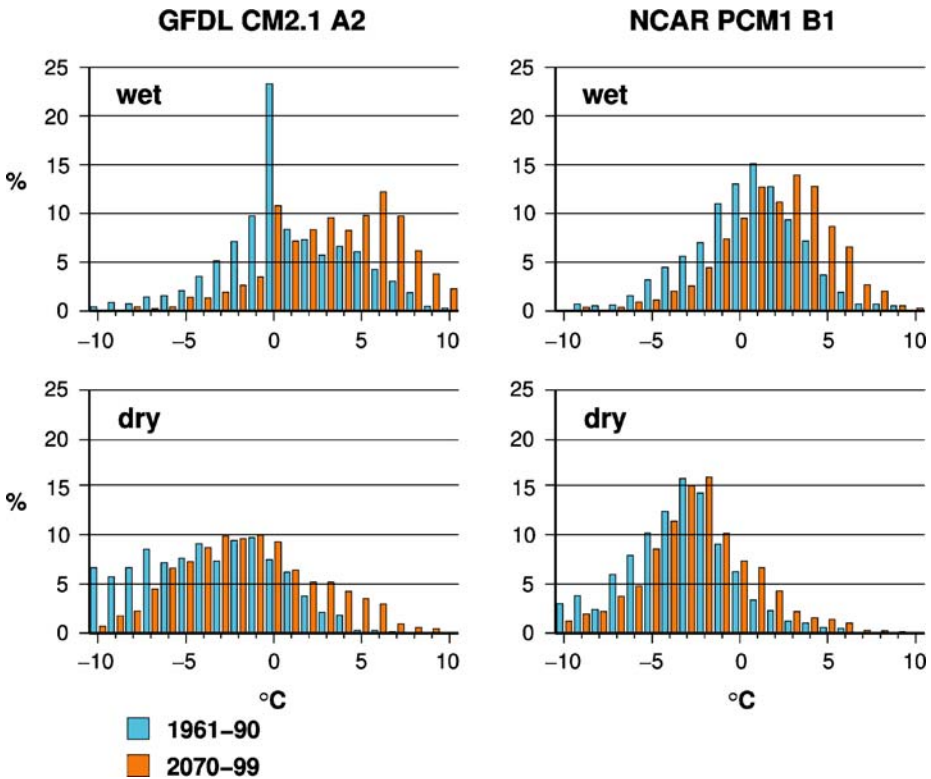


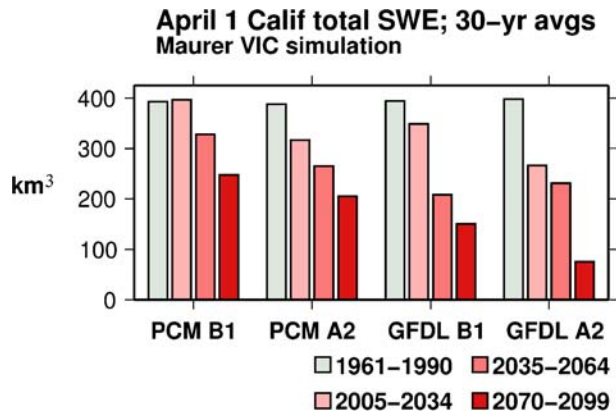
Fig. 12 Distribution, binned by 1°C intervals (percentages of total counts in the range from -10 to +10°C), of daily northern California minimum temperatures (Tmin) for November–March 1961–1990 (blue) and 2070–2099 (orange) on days that are dry, and on days with precipitation, from GFDL A2 (left) and PCM B1 (right) simulations

Table 5 Change in April 1 snow water equivalent, San Joaquin, Sacramento, and parts of Trinity drainages from VIC hydrologic model

	Mean 1961–1990	2005–2034		2035–2064				2070–2099					
		Change		Change		Change		Change		Change		Change	
		(%) PCM	(%) GFDL	(%) PCM	(%) GFDL	(%) PCM	(%) GFDL	(%) PCM	(%) GFDL	(%) PCM	(%) GFDL	(%) PCM	(%) GFDL
PCM		B1	A2	B1	A2	B1	A2	B1	A2	B1	A2	B1	A2
1,000–2,000 m elevation	4.0 km ³ (3.24 Maf)	-13	-35	-20	-48	-26	-52	-68	-61	-60	-76	-75	-93
2,000–3,000 m elevation	6.5 km ³ (5.27 Maf)	+12	-09	-04	-33	-08	-21	-36	-32	-25	-34	-56	-79
3,000–4,000 m elevation	2.49 km ³ (2.02 Maf)	+19	+01	+04	-13	-02	-05	-16	-11	-05	-02	-41	-55
All elevations	13.0 km ³ (10.54 Maf)	+06	-15	-07	-29	0.12	-27	-42	-37	-32	-41	-59	-79

Similar computations for HadCM3 A1fi and B1 simulations and for PCM A1fi simulation are presented in Tables 1 and 2 of Hayhoe et al. 2004. 1961–1990 mean snow water equivalent (SWE) given in km³ and in million acre feet (MAF).

Fig. 13 California statewide average April 1 snow water equivalents from 1961–1990, 2005–2034, 2035–2064, and 2070–2099 simulations of PCM B1 and A2, and GFDL B1 and A2 conditions



GHG-emitting (A2) scenario. By 2070–2099, virtually no snow is left below 1,000 m under this scenario. In terms of water storage volume, snow losses have greatest impact in relatively warm low-middle and middle elevations between about 1,000 and 2,000 m, with losses of 60 to 93% and between about 2,000 and 3,000 m, with losses of 25 to 79%. Because the highest elevations in the Sierra Nevada tend to be in the southern part of the range, the largest reductions in snow accumulation occur in the central and northern parts of the range (Fig. 14).

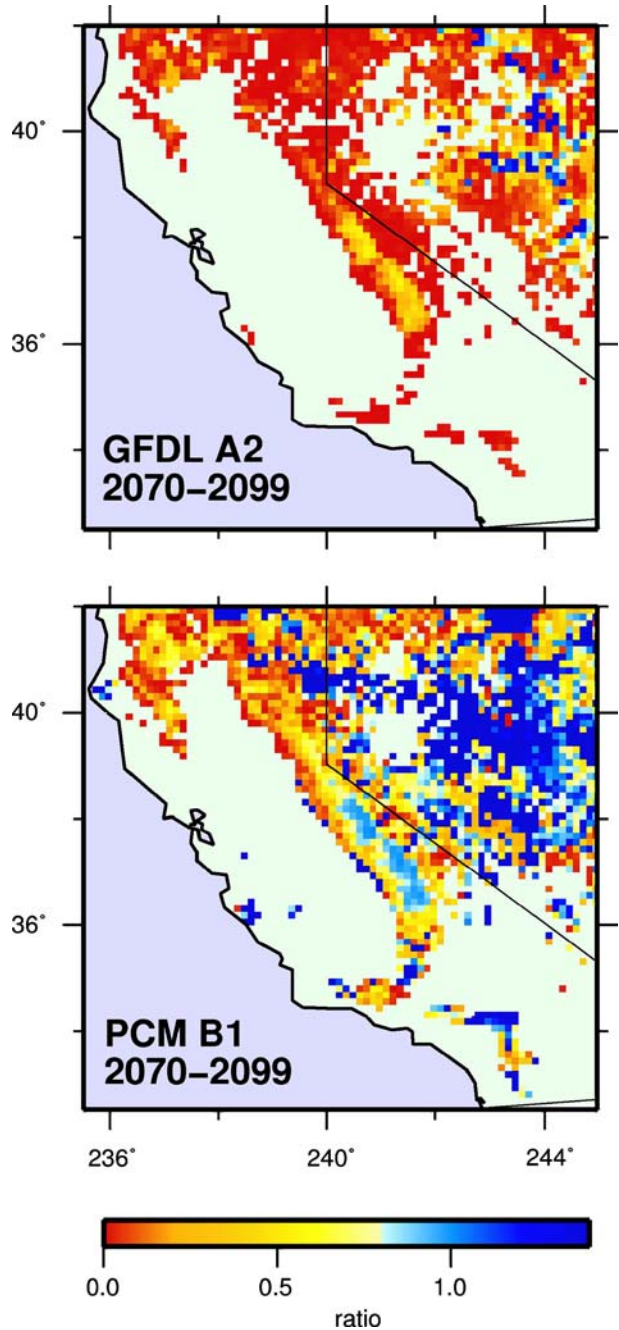
5 Discussion and summary

A purposely diverse set of possible twenty-first century climates for California were investigated to provide the context and drivers for an evaluation of possible drivers and impacts in a variety of sectors. The first-order surface climate variables, temperature and precipitation – and some immediate implications for snowpacks and runoff in the State, were the focus of the present study. The projections analyzed were based strictly on simulations by *global* climate models. Although regional models will be needed to distribute climate over the complex landscape of California, the first-order climate changes tend to derive from the large, indeed global, scale responses to increasing GHGs, even when considered at the California scale.

These projections that were the focus of the current study are mostly from two state-of-the-art global climate models forced (mostly) by two GHG emission scenarios. These projections are not “predictions,” but rather represent purposely diverse examples from among the many plausible climates that may occur in the twenty-first century. Future GHG concentrations are uncertain because they depend on future social, political, and technological decisions, and thus the IPCC has produced four “families” of emission scenarios (Houghton et al. 2001). To explore some of the range of futures expressed by the IPCC emissions scenarios, an A2 emissions scenario (with its medium-high emissions) and a B1 (low emissions) scenario were selected from the current IPCC Fourth climate-assessment archives for evaluation. The global climate model simulations focused upon here were from the NCAR/DOE group’s PCM1 model and GFDL’s CM2.1

Among these and all other IPCC projections, temperatures are projected to rise significantly during the twenty-first century. To put these into a more complete inter-model, interscenario context, some of the analyses used a much broader set of IPCC 4th

Fig. 14 Change in springtime snow accumulation from the VIC hydrological model, driven by climate changes from GFDL A2 and PCM B1 climate simulations. Changes are expressed as ratio of 2070–2099 April 1 snow water equivalent (*SWE*) to historical (1961–1990) *SWE*



Assessment Simulations, but future studies will need to consider this broader, probabilistic perspective more comprehensively.

The magnitude of projected warming varies from model to model, and, especially after the middle of the twenty-first century, from emission scenario to emission scenario.

California's temperatures rise, between 2000 and 2100, by 1.7 to 3.0°C in the lower range of projected warmings, 3.1 to 4.3°C in the medium range, and 4.4 to 5.8°C in the high range. Over this time period, the warming develops approximately linearly, and it is important to note that substantial warming has occurred even in the first 30 years of the century long period. Warming affects both wet and dry days to about the same degree.

Another way to think about these warming trends is in terms of the marked shifts they produce in the lower, middle and upper thirds of the historical temperature distributions. By 2070–2099, in all of the projections, temperature increases were sufficient to nearly eliminate seasonal mean temperatures in the lower third of the distribution and sharply reduce those in the middle third. Such climate changes would be, in the words of Hansen et al. 2007, “climate changes outside of the range of local experience.” A noteworthy feature in the temperature projections is that the warming through the twenty-first Century does not level off, especially in projections using the medium and high greenhouse gas emission scenarios, implying that California's climate would continue to warm in (at least) the subsequent decades of the twenty-second century.

There is little consensus among trends in the various precipitation projections for California during the next century. Instead, the large majority of the recent IPCC model projections, including several simulations not analyzed in detail here, yield relatively small (5–20%) change in total precipitation. It is worth emphasizing though, that a 10–20% change in annual precipitation is *not a minor* gain or loss. In the historical record, a 15% loss in precipitation is sufficient to cast a year into the lowest third of the annual totals, and, since runoff is a non-linear outcome of precipitation, lessening the supply in many cases drives runoff disproportionately lower.

Continued warming in California will have uneven effects on the California landscape. For example, warming will diminish snow accumulations by producing increased trends toward more rain and less snow, and earlier snowmelt, especially in lower to middle elevations of mountain catchments. Losses of snow, perhaps the early signs of climate change, are already being observed in the western United States, and hydrologic simulations indicate that the losses will increase as the warming increases. In the present study, the most severe losses are produced by the more sensitive CM2.1 model under the higher A2 (and A1fi) emissions. By 2070–2099, under the A2 and B1 emission scenarios in the PCM and GFDL models, losses of snow water equivalent (SWE) in the San Joaquin, Sacramento and Trinity drainages, as percentages of (1961–1990) historical averages, range from –32 to –79%. By 2070–2099, virtually no snow is left below 1,000 m under the A2 scenario in the GFDL model. Because higher elevation, and thus cooler, areas in the Sierra Nevada are mostly in the southern part of the range, the largest reductions in snow are projected to occur in the central and northern range.

Acknowledgments Support for DC, EM, MT and KH was provided by the State of California through the California Energy Commission PIER Program and the California Environmental Protection Agency. DC and MT were also supported by NOAA RISA Program through the California Applications Center and from DOE. MD's and DC's involvement were facilitated by the USGS Priority Ecosystems Study of the San Francisco Estuary. Kelly Redmond, Philip Mote and two anonymous reviewers provided careful reading of draft versions and thoughtful comments.

References

Abdulla FA, Lettenmaier DP, Wood EF, Smith JA (1996) Application of a macroscale hydrologic model to estimate the water balance of the Arkansas-Red River basin. *J Geophys Res* 101:7449–7459

- Barnett T, Malone R, Pennell W, Stammer D, Semtner A, Washington W (2004) The effects of climate change on water resources in the west: introduction and overview. *Clim Change* 62:1–11
- Cayan DR, Kammerdiener S, Dettinger MD, Caprio JM, Peterson DH (2001) Changes in the onset of spring in the western United States. *Bull Am Meteorol Soc* 82(3):399–415
- Cayan DC, Maurer E, Dettinger MD, Tyree M, Hayhoe K, Bonfils C, Duffy P, Santer B (2006) Climate scenarios for California. FINAL white paper from California Climate Change Center, publication # CEC-500-2005-203-SF, posted: March 15, 2006. http://www.climatechange.ca.gov/climate_action_team/reports/index.html
- Christensen NS, Wood AW, Voisin N, Lettenmaier DP, Palmer RN (2004) The effects of climate change on the hydrology and water resources of the Colorado River basin. *Clim Change* 62:337–363
- Cubasch U, Meehl GA, Boer GJ, Stouffer RJ, Dix M, Noda A, Senior CA, Raper S, Yap KS (2001) Projections of future climate change. In: Houghton JT, Yihui D, Noguier M (eds) *Climate change 2001: The scientific basis*. Cambridge University Press
- Delworth T et al (2006) GFDL's CM2 global coupled climate models – Part 1: Formulation and simulation characteristics. *J Climate* 19(5):643–674
- Dettinger MD (2005) From climate-change spaghetti to climate-change distributions for 21st Century California. *San Francisco Estuary and Watershed Science* 3(1): <http://repositories.cdlib.org/jmie/sfews/vol3/iss1/art4>
- Dettinger MD (2006) A component-resampling approach for estimating probability distributions from small forecast ensembles. *Clim Change* 76:149–168 DOI 10.1007/s10584-005-9001-6
- Dettinger MD, Battisti DS, Garreaud RD, McCabe GJ, Bitz CM (2001) Interhemispheric effects of interannual and decadal ENSO-like climate variations on the Americas. In: Markgraf V (ed) *Interhemispheric climate linkages: present and past climates in the Americas and their societal effects*. Academic, pp 1–16
- Field CB, Daily GC, Davis FW, Gaines S, Matson PA, Melack J, Miller NL (1999) *Confronting climate change in California: ecological impacts on the golden state*. Union of Concerned Scientists, Cambridge, MA
- Gershunov A, Douville H (2007) Extensive summer hot and cold extremes under current and possible future climatic conditions: Europe and North America. Assessing, modeling and monitoring the impacts of extreme climate events. Cambridge University Press (in press)
- Gordon C, Cooper C, Senior CA, Banks H, Gregory JM, Johns TC, Mitchell JFB, Wood RA (2000) The simulation of SST, sea ice extents and ocean heat transports in a version of the Hadley Centre coupled model without flux adjustments. *Clim Dyn* 16:147–168
- Hansen J, Sato Mki, Ruedy R, Nazarenko L, Lacis A, Lo K, Schmidt GA, Russell G, Aleinov I, Bauer M, Bauer S, Baum E, Bell N, Cairns B, Canuto V, Chandler M, Cheng Y, Cohen A, Del Genio A, Faluvegi G, Fleming E, Friend A, Hall T, Jackman C, Jonas J, Kelley M, Kiang N, Koch D, Labov G, Lerner J, Menon S, Miller RL, Novakov T, Oinas V, Perlwitz Ja, Perlwitz Ju, Rind D, Romanou A, Shindell D, Stone P, Sun S, Streets D, Tausnev N, Thresher D, Yao M, Zhang S (2007) Dangerous human-made interference with climate: A GISS modelE study. *Atmos Chem Phys* 7:2287–2312
- Hansen J, Ruedy R, Sato M, Lo K (2006) GISS surface temperature analysis: global temperature trends: 2005 Summation. <http://data.giss.nasa.gov/gistemp/2005/>
- Hayhoe K, Cayan D, Field CB, Frumhoff PC, Maurer EP, Miller NL, Moser SC, Schneider SH, Cahill KN, Cleland EE, Dale L, Drapek R, Hanermann RM (2004) Emissions pathways, climate change, and impacts on California. *Proc Natl Acad Sci USA* 101(34):12422–12427 24 August 2004
- Houghton JT et al (eds) (2001) *The scientific basis: contribution of working group I to the third assessment report of the intergovernmental panel on climate change*. Climate Change, Cambridge University Press, pp 525–582
- Jones P, Palutikof P (2006) Global temperature record. Climate research unit, University of East Anglia. <http://www.cru.uea.ac.uk/cru/info/warming/>
- Knowles N, Cayan DR (2002) Potential effects of global warming on the Sacramento/San Joaquin watershed and the San Francisco estuary. *Geophys Res Lett* 29(18):1891–1895
- Knowles N, Dettinger MD, Cayan DR (2007) Trends in snowfall versus rainfall in the Western United States. *J Climate* (in press)
- Knutson TR, Delworth TL, Dixon KW, Held IM, Lu J, Ramaswamy V, Schwarzkopf MD, Stenchikov G, Stouffer RJ (2006) Assessment of twentieth century regional surface temperature trends using the GFDL CM2 Coupled Models. *J Climate* 10:1624–1651
- Lettenmaier DP, Gan TY (1990) Hydrologic Sensitivities of the Sacramento-San Joaquin River Basin, California, to Global Warming, edited. *Water Resour Res* 69–86
- Liang X, Lettenmaier DP, Wood E, Burges SJ (1994) A simple hydrologically based model of land surface water and energy fluxes for general circulation models. *J. Geophys Res* 99(D7):14, 415–414, 428
- Liang X, Lettenmaier DP, Wood EF (1996) One-dimensional statistical dynamic representation of subgrid spatial variability of precipitation in the two-layer variable infiltration capacity model. *J Geophys Res* 101(D16):21, 403–421, 422

- Lohmann D, Nolte-Holube R, Raschke E (1996) A large-scale horizontal routing model to be coupled to land surface parameterization schemes. *Tellus* 48A:708–721
- Maurer EP (2007) Uncertainty in hydrologic impacts of climate change in the Sierra Nevada Mountains, California under two emissions scenarios. *Clim Change* 82:309–325
- Maurer EP, Duffy PB (2005) Uncertainty in projections of streamflow changes due to climate change in California. *Geophys Res Lett* 32:L03704
- Maurer EP, O'Donnell GM, Lettenmaier DP, Roads JO (2001) Evaluation of the land surface water budget in NCEP/NCAR and NCEP/DOE reanalyses using an off-line hydrologic model. *J Geophys Res* 106 (D16):17841–17862
- Maurer EP, Wood AW, Adam JC, Lettenmaier DP, Nijssen B (2002) A long-term hydrologically-based data set of land surface fluxes and states for the conterminous United States. *J Climate* 15(22):3237–3251
- Meehl GA, Washington WM, Wigley TML, Arblaster JM, Dai A (2003) Solar and greenhouse gas forcing and climate response in the twentieth century. *J Climate* 16(3):426–444
- Miller NL, Bashford KE, Strem E (2003) Potential impacts of climate change on California hydrology. *J Am Water Resour Assoc* 39:771–784
- Mote PW, Hamlet AF, Clark MP, Lettenmaier DP (2005) Declining mountain snowpack in western North America. *Bull Am Meteorol Soc* 86:39–49
- Nakic'enović N, Alcamo J, Davis G, de Vries B, Fenhann J, Gaffin S, Gregory K, Grubler A, Jung TY, Kram T et al (2000) Intergovernmental panel on climate change special report on emissions scenarios. Cambridge Univ. Press, Cambridge, U.K
- National Assessment Synthesis Team (2001) Climate change impacts on the United States. The potential consequences of climate variability and change, US Global Change Research Program
- Nijssen B, Lettenmaier DP, Liang X, Wetzel SW, Wood E (1997) Streamflow simulation for continental-scale basins. *Water Resour Res* 33:711–724
- Nijssen B, O'Donnell GM, Lettenmaier DP, Lohmann D, Wood EF (2001) Predicting the discharge of global rivers. *J Climate* 14(15):1790–1808
- Payne JT, Wood AW, Hamlet AF, Palmer RN, Lettenmaier DP (2004) Mitigating the effects of climate change on the water resources of the Columbia River Basin. *Clim Change* 62:233–256
- Pope VD, Gallani ML, Rowntree PR, Stratton RA (2000) The impact of new physical parameterisations in the Hadley Centre climate model – HadAM3. *Clim Dyn* 16:123–146
- Santer BD, Wigley TML, Barnett TP, Anyamba E (1996) Detection of climate change and attribution of causes. Cambridge University Press, New York, NY (USA)
- Stewart I, Cayan DR, Dettinger MD (2005) Changes towards earlier streamflow timing across western North America. *J Climate* 18:1136–1155
- Stouffer et al (2006) GFDL's CM2 global coupled climate models – Part 4: Idealized climate response. *J Climate* 19:723–740
- Tett SFB, Stott PA, Allen MR, Ingram WJ, Mitchell JFB (1999) Causes of twentieth century temperature change. *Nature* 399:569–572
- VanRheenen NT, Wood AW, Palmer RN, Lettenmaier DP (2004) Potential implications of PCM climate change scenarios for Sacramento-San Joaquin River Basin hydrology and water resources. *Clim Change* 62:257–281
- Washington WM, Weatherly JW, Meehl GA, Semtner AJ, Bettge TW, Craig AP, Strand WG, Arblaster J, Wayland VB, James R, Zhang Y (2000) *Clim Dyn* 16(10/11):755–774
- Wilson T et al (2003) Global climate change and California: potential implications for ecosystems, health, and the economy. California Energy Commission: Sacramento. 1*138. Available at http://www.energy.ca.gov/pier/final_project_reports/500-03-058cf.html
- Wood AW, Maurer EP, Kumar A, Lettenmaier DP (2002) Long-range experimental hydrologic forecasting for the eastern United States. *J Geophys Res* 107(D20):4429
- Wood AW, Leung LR, Sridhar V, Lettenmaier DP (2004) Hydrologic implications of dynamical and statistical approaches to downscaling climate model outputs. *Clim Change* 62:189–216
- World Meteorological Organization (WMO) (2005) Statement on the Status of the Global Climate in 2005: Geneva, 15 December, 2005. <http://www.wmo.ch/index-en.html>
- Zhao R-J, Fang L-R, Liu X-R, Zhang Q-S (1980) The Xinanjiang model, in *Hydrological Forecasting, Proceedings, Oxford Symposium*, edited, pp 351–356, IAHS Publ. 129